

Identification of the Heat Equation Parameters for Estimation of a Bare Overhead Conductor's Temperature by the Differential Evolution Algorithm

Authors:

Mirza Sarajli?, Jože Pihler, Nermin Sarajli?, Gorazd Štumberger

Date Submitted: 2018-09-21

Keywords: Optimization, Simulation, measurement, conductor temperature, parameter identification, overhead transmission line

Abstract:

This paper deals with the Differential Evolution (DE) based method for identification of the heat equation parameters applied for the estimation of a bare overhead conductor's temperature. The parameters are determined in the optimization process using a dynamic model of the conductor; the measured environmental temperature, solar radiation and wind velocity; the current and temperature measured on the tested overhead conductor; and the DE, which is applied as the optimization tool. The main task of the DE is to minimise the difference between the measured and model-calculated conductor temperatures. The conductor model is relevant and suitable for the prediction of the conductor temperature, as the agreement between measured and model-calculated conductor temperatures is exceptional, where the deviation between mean and maximum measured and model-calculated conductor temperatures is less than 0.03 °C.

Record Type: Published Article

Submitted To: LAPSE (Living Archive for Process Systems Engineering)

Citation (overall record, always the latest version):

LAPSE:2018.0583

Citation (this specific file, latest version):

LAPSE:2018.0583-1

Citation (this specific file, this version):


LAPSE:2018.0583-1v1

DOI of Published Version: <https://doi.org/10.3390/en11082061>

License: Creative Commons Attribution 4.0 International (CC BY 4.0)

Article

Identification of the Heat Equation Parameters for Estimation of a Bare Overhead Conductor's Temperature by the Differential Evolution Algorithm

Mirza Sarajlić ^{1,*} , Jože Pihler ¹, Nermin Sarajlić ² and Gorazd Štumberger ¹

¹ Faculty of Electrical Engineering and Computer Science, University of Maribor, 2000 Maribor, Slovenia; joze.pihler@um.si (J.P.); gorazd.stumberger@um.si (G.Š.)

² Faculty of Electrical Engineering, University of Tuzla, 75000 Tuzla, Bosnia and Herzegovina; nermin.sarajlic@untz.ba

* Correspondence: mirza.sarajlic@um.si; Tel.: +386-2-220-7086

Received: 17 July 2018; Accepted: 6 August 2018; Published: 8 August 2018



Abstract: This paper deals with the Differential Evolution (DE) based method for identification of the heat equation parameters applied for the estimation of a bare overhead conductor's temperature. The parameters are determined in the optimization process using a dynamic model of the conductor; the measured environmental temperature, solar radiation and wind velocity; the current and temperature measured on the tested overhead conductor; and the DE, which is applied as the optimization tool. The main task of the DE is to minimise the difference between the measured and model-calculated conductor temperatures. The conductor model is relevant and suitable for the prediction of the conductor temperature, as the agreement between measured and model-calculated conductor temperatures is exceptional, where the deviation between mean and maximum measured and model-calculated conductor temperatures is less than 0.03 °C.

Keywords: overhead transmission line; conductor temperature; parameter identification; measurement; simulation; optimization

1. Introduction

The main task of the overhead conductor is the transmission of electricity. Due to the trend of increased consumption and interstate exchange of electricity, the transmission companies are faced with the problem of the phase conductor thermal loading [1]. To control the thermal loading, the operator of the transmission network has to perform continuous acquisition of conductor temperature measurements, measurements of climatic conditions in the vicinity of the route and predict the course of the conductor thermal load and the electricity transmission capability. The energy that is transported depends on the type of load, the current and the environmental conditions. When talking about the influence of the environment on the conductor temperature, the environmental temperature, the wind velocity and the solar radiation, are the most important factors. The conductor temperature is important when it comes to the conductor sagging. The temperature influences the conductor sagging directly and, through it, the clearances, that must be inside prescribed limits along the entire power line in all loading conditions. Thus, the ability to predict the conductor temperature, sagging and clearances in all power line spans is crucial for determining maximal power line loading under given operation conditions.

Several studies deal with analytical numerical methods for assessing the temperature of overhead power line conductors [1–10], where environmental conditions and heat-balance equations have been applied [11,12].

The authors in [1] talk about the environmental impacts on the conductor temperature and system development for the monitoring of these factors. Two different methods were used for calculating the maximum conductor temperature under different conditions in [2]. Analytical and empirical formulas are used for the iterative technique and the numeric method, that is based on the finite volume resolution technique. The authors in [3] determine the maximal loading using conductor temperature measurements and Dynamic Line Rating (DLR) methodology. [4] deals with the time dependent thermal analysis of an overhead transmission line and a buried electric power cable. The temperature is calculated as a function of time using real input data. The algorithm for the calculation of the temperature fluctuations along an overhead transmission power line is described in [5]. The authors in [6] deal with the external factors that influence the conductor temperature. A simulation model has been developed, where the thermal behaviour of the conductor is simulated under static and dynamic operating conditions. The objective was to determine the maximum current that can flow through the conductor without exceeding the temperature limit of the conductor. The principal component regression based method is used in [7] to predict the Dynamic Thermal Rating (DTR) of power lines by using the weather data forecast by meteorological stations. The conductor temperature is predicted in [8] by comparing the calculated temperatures with the measured ones to improve the accuracy of the dynamic thermal circuit rating (DTCR) systems. Echo State Network (ESN) is used in [9] to predict the conductor thermal dynamics under various weather conditions from historical data. Instead of calculating the conductor temperature directly. In [10], the conductor temperature is calculated considering the environmental factors and power flow. Based on the known conductor temperature, they have calculated the sag and the conductor resistance and losses.

CIGRE (International Council on Large Electric Systems) and IEEE (Institute of Electrical and Electronics Engineers) have Standards to calculate the conductor temperature [13–15]. Both of the Standards use a basic heat balance equation but then their approach to calculating the heat balance is different [16,17].

To the best knowledge of the authors, no heat equation parameter-determining technique for electric overhead power lines, based on optimization, measured data and heat balance equation, have been published so far. Hence, the main novelty of this paper is a parameter identification technique based on the Differential Evolution (DE) algorithm, a heat equation based dynamic model and time behaviour of measured data. Any optimization method such as Particle Swarm Optimization (PSO) [18], genetic algorithm [19] or other, could be used in the optimization process. In this paper the DE, a stochastic optimization algorithm, which has proved to be very suitable for solving of nonlinear and constrained real life optimization problems in engineering [20–27], has been used. The goal of the DE algorithm is to reach the best possible agreement between the measured and heat equation calculated conductor temperature time behaviours under dynamic operating conditions. The objective function to be minimised is the root mean square difference between the measured and calculated conductor temperatures. The DE based method for identifying the heat equation parameters is confirmed through the comparison of measured and calculated time behaviours of conductor temperatures for two cases of bare overhead conductors. An excellent agreement between the measured and calculated conductor temperature dynamic behaviours is achieved when the parameters of the heat equation determined by the DE are used in the heat equation based dynamic model.

The paper is organised in 6 sections. Section 2 provides a description of a conductor dynamic model. Section 3 proposes a method for determining heat equation parameters based on the time behaviours of measured data, dynamic model and DE optimization algorithm. Section 4 describes performed measurements and the experimental setup. The parameters obtained by DE and comparison between the model calculated and measured conductor temperatures are presented in Section 5, whilst Section 6 concludes the paper.

2. Conductor Dynamic Model

The temperature of an overhead conductor depends on the thermal balance of incoming and outgoing heat [1,13,15]. The basic equation that describes the conductor temperature at the given time instant t can be written in differential form (1):

$$p_j(t) + p_s(t) + p_i(t) = p_c(t) + p_r(t) + p_w(t) + mc_p \frac{dT_s}{dt}, \quad (1)$$

where $p_j(t)$ [W/m] is the conductor heating due to the joule losses of the conductor; $p_s(t)$ [W/m] is the conductor heating due to the solar radiation; $p_i(t)$ [W/m] is the conductor heating due to the corona effect; $p_c(t)$ [W/m] is the conductor convective cooling; $p_r(t)$ [W/m] is the conductor radiative cooling; $p_w(t)$ [W/m] is the evaporative cooling, m [kg/m] is the conductor mass per meter, c_p [J/kgK] is the specific heat of the conductor at the constant pressure and $T_s(t)$ [°C] is the conductor temperature. In this paper, the $p_i(t)$ and $p_w(t)$ are neglected due to their insignificant influence on the result [13]. Considering this, the Equation (1) can be rewritten in the integral form (2):

$$T_s(t) = T_s(t_0) + \frac{1}{mc_p} \int_{t_0}^t (p_j(\tau) + p_s(\tau) - p_c(\tau) - p_r(\tau)) d\tau, \quad (2)$$

where $T_s(t_0)$ is the initial temperature at the time instant t_0 , $[t_0, t]$ is the time interval of observation, whilst τ is the auxiliary variable. In the next subsections, the individual terms in (2) are described. Figure 1, similar to the one in [15], shows overhead conductor heating and cooling.

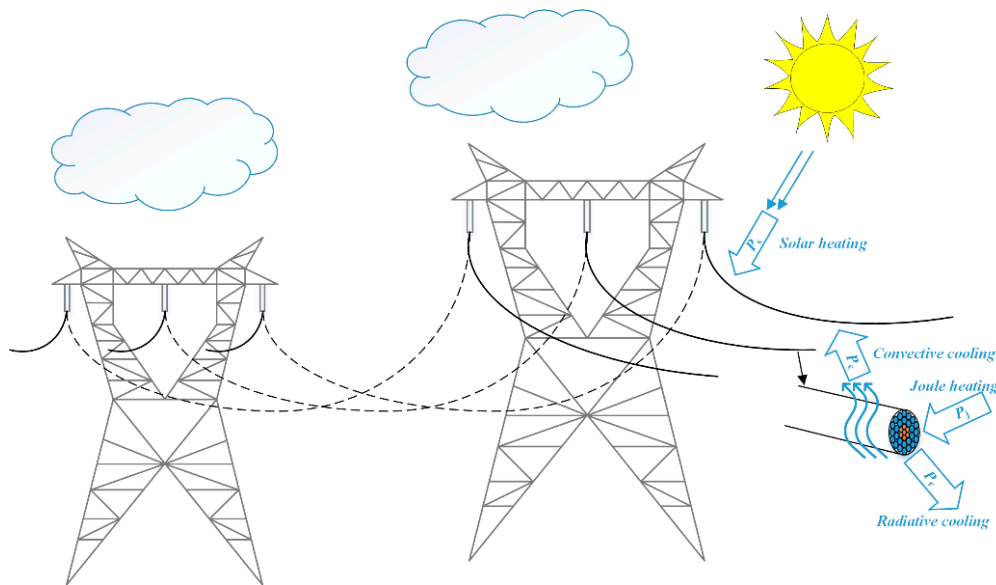


Figure 1. Overhead conductor heating and cooling.

2.1. The Influence of the Joule Losses on the Conductor Temperature

Joule losses present the main heat source in the heat balance Equations (1) to (2). The conductor heating due to the joule losses $p_j(t)$ [W/m] are described by (3) [13], where $i(t)$ [A] is the AC current instantaneous value at the time instant t ; r_{20} is the mean value of the conductor resistance on the unit length at 20 °C [Ω/m]; α_{20} is the temperature coefficient at 20 °C [1/K]; $T_s(t)$ is the conductor temperature at the time instant t .

$$p_j(t) = \left(i(t) \cdot \sqrt{1.0123 + 2.36 \cdot 10^{-5} \cdot i(t)} \right)^2 \cdot r_{20} \cdot (1 + \alpha_{20} (T_s(t) - 20 \text{ °C})). \quad (3)$$

The conductor resistance value r_{20} is defined by the conductor. Two types of bare overhead conductors are discussed in this paper: Aluminum Conductor Steel Reinforced (AlFe) 490/65 (Faculty of Electrical Engineering and Computer Science, Maribor, Slovenia) and AlFe 240/40. Their r_{20} values are 0.059 and 0.119, respectively [28]. However, they both have the same α_{20} value, which is 0.0052 [28].

2.2. Solar Heating of the Conductor

The conductor heating due to solar radiation $p_s(t)$ [W/m] is described by (4), where is the absorptivity factor of the conductor; $H(t)$ [W/m²] is the solar radiation at the time instant t and d [m] is the diameter of the conductor. The value of the absorptivity factor β is between 0.27 and 0.95 [13].

$$p_s(t) = 1000 \cdot \beta \cdot H(t) \cdot d. \quad (4)$$

2.3. Convective Cooling of the Inductor

Convective cooling of the conductor can be forced or natural [13]. The direction and wind velocity determine whether the conductor is cooling by forced or natural convection. The following equation describes forced convective cooling:

$$p_c(t) = 1000 \cdot \pi \cdot \lambda_f(t) \cdot (T_s(t) - T_a(t)) \cdot Nu, \quad (5)$$

where $p_c(t)$ [W/m] is the conductor convective cooling; $\lambda_f(t)$ [W/mK] is the thermal conductivity of air; $T_s(t)$ [°C] is the conductor temperature; $T_a(t)$ [°C] is the ambient temperature. All the aforementioned variables are given for the time instant t , whilst Nu is the Nusselt number [13].

The thermal conductivity of air $\lambda_f(t)$ is given by (6) [13]:

$$\lambda_f(t) = 2.42 \cdot 10^{-2} + 7.2 \cdot 10^{-5} \cdot T_f(t), \quad (6)$$

where $T_f(t)$ is defined by (7):

$$T_f(t) = 0.5 \cdot (T_s(t) + T_a(t)). \quad (7)$$

2.4. Radiative Cooling of the Conductor

The heat transfer due to radiation is described by Stefan-Boltzmann's law. Based on this law, the radiative cooling of the conductor $p_r(t)$ [W/mm] can be described by (8):

$$p_r(t) = 1000 \cdot \pi \cdot d \cdot \varepsilon \cdot \sigma_{sb} \cdot \left[(T_s(t) + 273.15)^4 - (T_a(t) + 273.15)^4 \right], \quad (8)$$

where d [m] is the diameter of the conductor; σ_{sb} is Stefan-Boltzmann's constant [13], that is $5.67 \cdot 10^{-8}$ [W/(m²·K⁴)]; ε is the emissivity factor of the conductor, which is in the range from 0.23 to 0.98 [13]. The conductor temperature and the ambient temperature at the time instant t are denoted with $T_s(t)$ [°C] and $T_a(t)$ [°C] respectively, whilst 273.15 is the conversion factor between the Kelvin [K] and Celsius [°C] temperature scales.

2.5. Calculation of the Conductor Temperature

The Equation (2) can be written in the following form:

$$T_s(t) = T_s(t - \Delta t) + \frac{1}{mc_p} \int_{t-\Delta t}^t (p_j(\tau) + p_s(\tau) - p_c(\tau) - p_r(\tau)) d\tau, \quad (9)$$

where Δt is the time between two samples that is coincident with the integration step. The value of Δt is 1 min.

Using the explicit forward Euler method (10), where $y(t)$ and $y(t - \Delta t)$ are the values of the function y in two consequent time steps, whilst $y'(t - \Delta t)$ is the time derivative of the function at time instant $t - \Delta t$, Equation (9) can be written in the form (11) and, further, in the recursive form (12). In (12) the index i denotes the current time step, whilst $i - 1$ denotes the previous time step.

$$y(t) = y(t - \Delta t) + \Delta t \cdot y'(y(t - \Delta t), t - \Delta t), \quad (10)$$

$$T_s(t) = T_s(t - \Delta t) + \Delta t \cdot \frac{1}{mc_p} \cdot (p_j(t - \Delta t) + p_s(t - \Delta t) - p_c(t - \Delta t) - p_r(t - \Delta t)), \quad (11)$$

$$T_{s,i} = T_{s,i-1} + \Delta t \cdot \frac{1}{mc_p} \cdot (p_{j,i} + p_{s,i} - p_{c,i} - p_{r,i}), \quad (12)$$

The operation of the conductor dynamic model has been tested with the catalogue parameter values from Table 1. The measurement results (conductor current, environmental temperature, solar radiation, wind velocity) have been used as input data for (3), (4), (5) and (8). The measurements have been carried out on the bare overhead conductors AlFe 240/40 and AlFe 490/65, which are described in Section 4. The conductors' catalogue data are shown in Table 6 (Section 4). The measured and model-calculated values of the conductor temperatures are compared, where the catalogue data for heat transfer parameters were applied in (3) to (8). The obtained results are shown in Tables 2 and 3. There are presented the mean and maximum values of the conductor temperatures for the conductors AlFe 490/65 and AlFe 240/40, operating at temperatures around 60 °C and 80 °C.

Table 1. Conductor model parameters from the catalogue [29].

Parameter	Value	
	AlFe 490/65	AlFe 240/40
α_{20} [1/K]		0.0052
r_{20} [Ω /km]	0.059	0.119
β		0.27
Nu		15
ε		0.23

Table 2. Measured (meas.) and model-calculated (calc.) mean and maximum values of the conductor temperature, heating and cooling powers (per unit values) for the conductor AlFe 490/65 and AlFe 240/40 at operating temperature 60 °C.

Operating Temperature 60 °C		Mean Value			Maximum Value		
		Meas.	Calc.	Meas. – Calc.	Meas.	Calc.	Meas. – Calc.
AlFe 490/65	T_s [°C]	55.42	55.9	0.48	60.69	61	0.31
	P_j [p.u.]	1	1	0	1	1	0
	P_s [p.u.]	1	0.66	0.34	1	0.54	0.46
	P_c [p.u.]	1	0.88	0.12	1	0.89	0.11
	P_r [p.u.]	1	0.54	0.46	1	0.54	0.46
AlFe 240/40	T_s [°C]	56.74	57	0.26	61.87	62	0.13
	P_j [p.u.]	1	1	0	1	1	0
	P_s [p.u.]	1	0.54	0.46	1	0.54	0.46
	P_c [p.u.]	1	0.88	0.12	1	0.88	0.12
	P_r [p.u.]	1	5.39	4.39	1	0.54	0.46

Table 3. Measured (meas.) and model-calculated (calc.) mean and maximum values of the conductor temperature, heating and cooling powers (per unit values) for the conductor AlFe 490/65 and AlFe 240/40 at operating temperature 80 °C.

Operating Temperature 80 °C		Mean Value			Maximum Value		
		Meas.	Calc.	Meas. – Calc.	Meas.	Calc.	Meas. – Calc.
AlFe 490/65	T_s [°C]	70.85	71	0.15	81.08	81.8	0.72
	P_j [p.u.]	1	1	0	1	1	0
	P_s [p.u.]	1	0.54	0.46	1	0.54	0.46
	P_c [p.u.]	1	0.88	0.12	1	0.88	0.12
	P_r [p.u.]	1	0.55	0.45	1	0.54	0.46
AlFe 240/40	T_s [°C]	78.39	78.9	0.51	81.54	81.7	0.16
	P_j [p.u.]	1	1	0	1	1	0
	P_s [p.u.]	1	0.54	0.46	1	0.54	0.46
	P_c [p.u.]	1	0.88	0.12	1	0.88	0.12
	P_r [p.u.]	1	0.54	0.46	1	5.42	4.42

The results presented in Tables 2 and 3 show clearly that the deviations between mean and maximum measured and model-calculated heating and cooling powers are between 0.11 and 4.42, which could be considered as inadequate and requiring improvements. On the other hand, the deviations between mean and maximum measured and model-calculated conductor temperatures are between 0.13 and 0.72. This deviation is tolerable. However, when a power system operates close to its limits, accurate prediction of maximal available loading for individual power lines and their conductors, considering actual climate conditions along these power lines, could be crucial to preserving power system stability. Conductor dynamic model works well as long as the conditions for heat balance are unchanged. In case of water, ice or snow coating on conductors, the heat balance changes. In that case, the increase of heat and temperature is preferred as it helps to melt snow or ice.

Thus, the main idea of this paper is to reduce the deviations between mean and maximum measured and calculated conductor temperatures, as well as heating and cooling powers, in order to improve the accuracy of predicted maximal available power line loading. This is done in the proposed DE based optimization procedure, where the measured data and conductor heating model (2) to (12) are used together in order to determine those values of parameters α_{20} , r_{20} , β , Nu and ε in (3) to (8), where the sum of squared differences between the time behaviours of measured and calculated conductor temperatures is minimal. The applied optimization tool, DE, is described briefly in the next section.

3. Determination of the Conductor Temperature Using DE

3.1. Differential Evolution

DE is a fast and robust population-based direct-search stochastic optimization algorithm, that was first introduced by Storn and Price [27]. This algorithm is popular with the engineering audience [20–22,24–26]. It is considered to be one of the best stochastic optimization methods for solving real-life engineering problems due to its satisfactory properties. DE is robust in reaching global minima [20], suitable for solving nonlinear and constrained optimization problems. It requires only boundaries of expected solutions and has only a few control parameters to be defined.

This paper carried out a MATLAB (Mathworks, version R2017a, Faculty of Electrical Engineering and Computer Science, Maribor, Slovenia) implementation of the variant DE/rand-to-best/1/exp in estimating the heat equation parameters for prediction of bare overhead conductor temperatures. Detailed descriptions of the DE algorithm are available in [23,27]. The optimization objective was the best possible agreement between the measured and dynamic model calculated time behaviours of conductor temperature. In order to reach the objective, the DE was changing values of the model parameters during the optimization procedure, therefore minimising the squared differences between the measured and calculated conductor temperatures. Table 4 presents the used DE settings.

Table 4. DE settings.

Parameter	Value
Number of parameters D	6
Population size NP	30
Weighting factor F	0.5
Crossover constant CR	0.7
Maximum number of iterations $iter_{max}$	250

The usage of DE in the process of determining the heat equation parameters of the bare overhead conductor requires proper tests performed on the tested bare overhead conductor and definition of the objective function, whose value is minimised in the optimization process.

3.2. Determining Parameters

DE determines the heat equation parameters α_{20} , r_{20} , β , Nu and ε from (3) to (8). The goal of optimization is the best possible agreement between the measured and calculated time behaviours of conductor temperatures. The quality of model parameters is evaluated by the objective function that is minimised in the optimization procedure. The optimization goal is to find that set of model parameters that ensures the best agreement between the measured and calculated time behaviours of conductor temperatures measured by the sum of their squared differences.

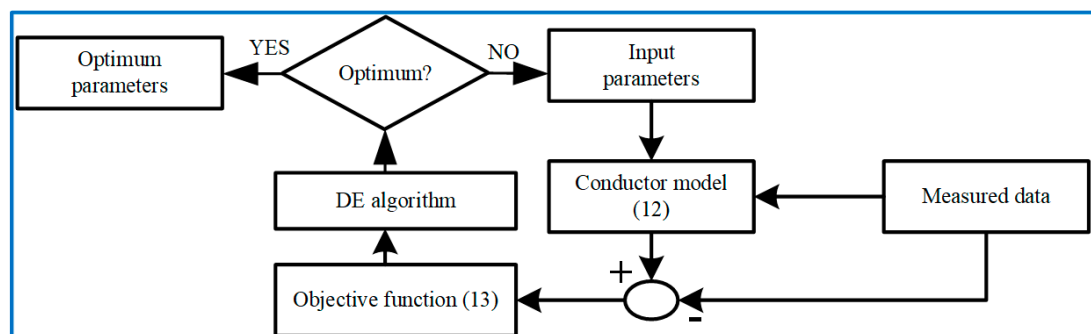
During the optimization process, the DE is searching for values of individual model parameters by minimising the value of the objective function q (13):

$$q = \sum_{i=1}^n e_{Tsi}^2 \quad (13)$$

where e_{Tsi} (14) is the difference between the measured (T_{s_meas}) and calculated (T_{s_calc}) conductor temperatures, whilst n is the number of iterations.

$$e_{Tsi} = T_{si_meas} - T_{si_calc} \quad (14)$$

The procedure for determining the conductor model's parameters presented in Figure 2 is organised as follows. In the first iteration, the DE algorithm generates a population of NP individuals, where NP is the size of the population. According to the DE rules, these individuals are considered as parents for the next generation. Those newly generated individuals that reach better objective function than their parents, replace their parent in the next generation. In this way, the objective function values of individuals are improved from generation to generation, mimicking evolution in nature.

**Figure 2.** Schematic presentation of procedure for determining the parameters.

Nu and ε . Each individual (set of parameter values) is applied in the conductor model, where the conductor temperature is calculated. The quality of the parameter set (individual) is evaluated by the objective function (13) as the sum of squared differences between the measured and calculated temperature time behaviours. The individual that reaches a sufficiently small and predefined value of the objective function is considered as the wanted solution. If the objective function value is not sufficiently small, the DE algorithm generates a new generation of individuals by using operators like crossover, mutation and selection [23,27]. The entire process repeats until the algorithm reaches the maximum number of generations, the objective function value has not been improved during a predefined number of generations, or the desired value of the objective function is reached. Figure 2 shows the implementation of DE in determining the conductor model parameters. According to the described procedure, the DE determines the parameters of the conductor dynamic model. The measured time series of the environmental temperature, solar radiation, wind velocity and conductor current are used in the dynamic model to calculate the time series of the conductor temperature. The differences of measured and calculated conductor temperature time series (14) are afterwards used in the objective function (13) which evaluates the quality of the conductor dynamic model parameter set. The DE searches for the set of conductor model parameters in a procedure, where the objective function value q (13) is minimized. Table 5 presents the maximum and minimum values of optimization variables.

Table 5. Minimum and maximum values of optimization variables.

Parameter	Minimum Value		Maximum Value	
α_{20} [1/K]	0.0035		0.0078	
r_{20} [Ω /km]	AlFe 490/65 0.059	AlFe 240/40 0.119	AlFe 490/65 0.0885	AlFe 240/40 0.1785
β	0.27		0.95	
Nu	11		25	
ε	0.23		0.98	

4. Experimental Set-Up and Measurements

The tests have been carried out on the testing site (field testing) (Figure 3) at different atmospheric conditions during different seasons (summer, autumn, winter). The applied experimental set-up consists of the testing line with overhead conductors, data acquisition system and supply system.

The test objects were bare overhead conductors AlFe 490/65 and AlFe 240/40 with the data shown in Table 6. The tests have been performed on the conductors for two operating temperatures 60 °C and 80 °C. Figure 4 shows an outline for the conductor AlFe 240/40.

Table 6. Parameters for conductors AlFe 490/65 and AlFe 240/40 [28,29].

Nominal cross-section of the conductor A [mm ²]	240/40	490/65
Calculated section of the conductor A [mm ²]	282.5	553.9
Number of Al wires	26	54
Number of Al layers	2	3
Diameter of Al wires [mm]	3.45	3.4
Calculated section A_{Al} [mm ²]	243	490.3
Number of Fe wires	7	7
Diameter of Fe wires [mm]	2.68	3.4
Calculated section A_{Fe} [mm ²]	39.5	63.6
Sectional ratio ε'	6	7.7
Outer diameter of the conductor d [mm]	21.8	30.6
Weight of the conductor [kg/km]	990	1866

The testing system contains a weather station for the acquisition of weather parameters (environmental temperature, solar radiation, wind velocity); a system for measuring the conductor temperature and a system for the conductor's current control.

The system for the conductor's current control enables fine tuning of the current. A proper setting of reference values for the current controller provides the conductor's operating temperature around 60 °C or 80 °C.

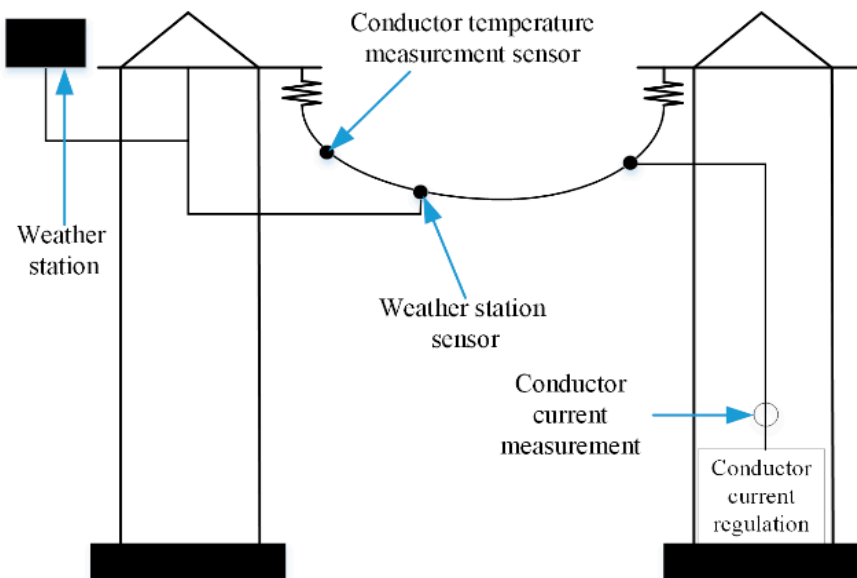


Figure 3. Schematic presentation of the testing site.

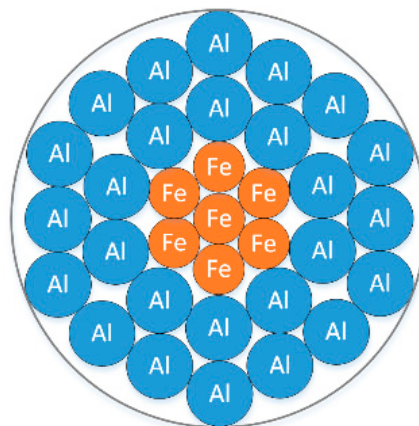


Figure 4. AlFe 240/40 conductor outline.

Figure 5 shows an example of measurements of the environmental temperature, current that flows through the conductor, solar radiation and wind velocity. The weather conditions and the current value in Figure 4 are given for the winter season. During the test, the temperature was below freezing. It was cloudy with wind velocity around 1 m/s. The test lasted 7 h and 26 min. Table 7 contains mean and maximum values of the data shown in Figure 5.

The measurements on the conductors AlFe 240/40 and AlFe 490/65, operating at temperatures 60 °C and 80 °C, were performed under different weather conditions, which are summarised in Table 8. In all the measurements performed, the sampling time was 1 min.

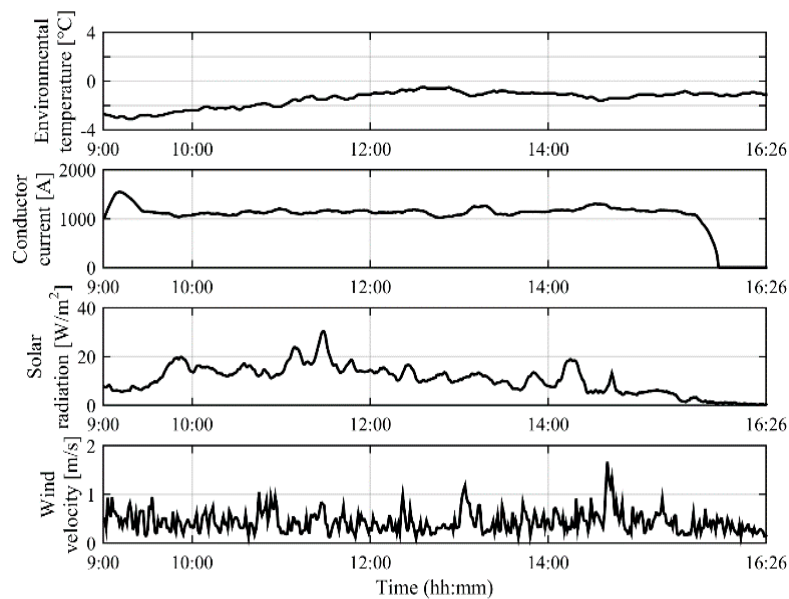


Figure 5. Measured weather data and conductor current.

Table 7. Data values from Figure 5.

	Mean Value	Maximum Value
Environmental temperature T_{env} [°C]	−1.38	−0.50
Conductor current I_{cond} [A]	1142.95	1308.46
Solar radiation H [W/m ²]	11.97	30.30
Wind velocity v_{wind} [m/s]	0.44	1.67

Table 8. Measurements results.

				Mean Value	Maximum Value	
Conductor AIFe 240/40	Measurement 1	Operating temperature [°C]	60	T_{env} [°C]	10.98	11.41
		Season	Autumn	I_{cond} [A]	725.25	904.88
		Time of measurement	7:48 to 16:25	H [W/m ²]	37.27	120.91
	Measurement 2	Operating temperature [°C]	80	T_{env} [°C]	31.12	34.3
		Season	Summer	I_{cond} [A]	759.04	902.77
		Time of measurement	9:00 to 16:35	H [W/m ²]	747.54	894.27
Conductor AIFe 490/65	Measurement 3	Operating temperature [°C]	60	T_{env} [°C]	−1.38	−0.5
		Season	Winter	I_{cond} [A]	1142.95	1308.46
		Time of measurement	9:00 to 16:27	H [W/m ²]	11.97	30.30
	Measurement 4	Operating temperature [°C]	80	T_{env} [°C]	32.79	35.5
		Season	Summer	I_{cond} [A]	831.35	1192.18
		Time of measurement	9:15 to 18:00	H [W/m ²]	628.46	866.64
		Duration of measurement	8 h and 45 min	v_{wind} [m/s]	1.03	2.87

The values of the environmental temperature, conductor current, solar radiation and wind velocity, measured on the conductors AIFe 240/40 and AIFe 490/65, operating at temperatures of approximately

60 °C and 80 °C, are presented in Table 8. They are used as the input data in the process of heat equation parameter identification. An example of the input data values (environmental temperature, conductor current, solar radiation, wind velocity and measured conductor temperature) is added as a Supplementary Material in the form of a table (Table S1).

5. Results

The proposed DE based method for determining heat equation parameter is conformed through the comparison of measured and calculated results. The measured time behaviours of current, environmental temperature, solar radiation, wind velocity and conductor temperature were applied in the proposed DE based optimization procedure in order to determine the heat equation parameters. The catalogue data of the parameters, shown in Table 1, are used to determine the optimization bounds. The results obtained by the proposed method are shown in Table 9 as the mean values of 10 subsequently performed optimization procedures. They are given for the conductors AlFe 490/65 and AlFe 240/40 operating at the temperature of approximately 60 °C.

Table 9. Conductor model parameters determined in the proposed optimization procedure.

Parameter	Value after Optimization		Value before Optimization	
	AlFe 490/65	AlFe 240/40	AlFe 490/65	AlFe 240/40
α_{20} [1/K]		0.0052		0.0052
r_{20} [Ω /km]	0.059	0.119	0.059	0.119
β		0.51		0.27
Nu		16.55		15
ε		0.57		0.23

Table 9 shows that the values of α_{20} and r_{20} after performed optimization are the same as the ones given in the catalogue [29]. On the other hand, the values of β and ε after optimization are in the middle of their minimum and maximum values defined in Table 7. The value of Nu after optimization is slightly bigger than the one given in Table 1.

The heat equation parameter values, determined by the proposed method and shown in Table 9, were used in all calculated results that follow.

The comparison between measured temperature (blue coloured line) and model calculated temperature using the catalogue parameters (red coloured line) and parameters determined by the proposed optimization procedure (yellow coloured line) is shown on the section of interval in Figure 6. Table 10 shows the values of those temperatures, where the difference can be seen between model calculated temperature using catalogue and identified parameters.

Since the main goal of objective function is to minimise the root mean square difference between the measured and model-calculated conductor temperature, the difference between the temperatures in Figure 6 and Table 10 is preferred to be minimal in order to show the working of the model and proposed method. The difference between measured and model-calculated using the catalogue parameters and parameters identified by the proposed optimization procedure is best seen at the section of interval of the heating powers (Figure 7).

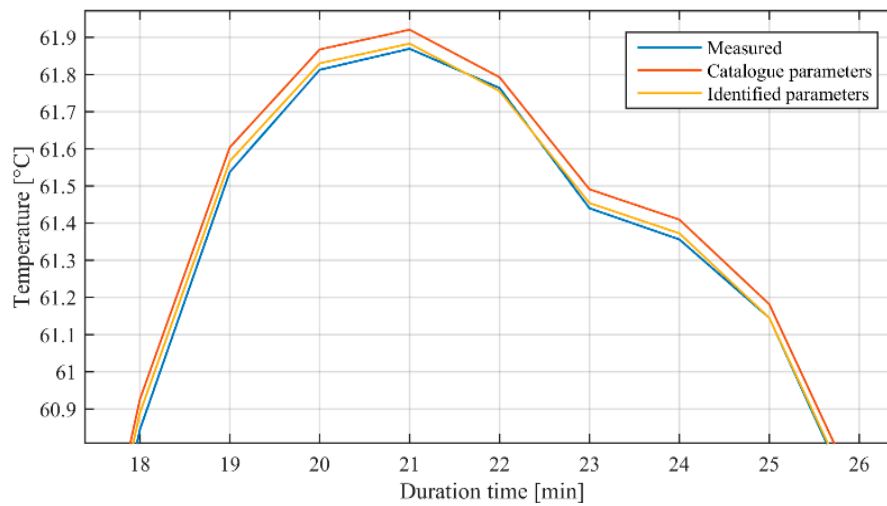


Figure 6. Measured (blue line) and model calculated temperature using catalogue parameters (red line) and parameters determined by the proposed optimization procedure (yellow line) at the conductor temperature 60 °C for the conductor A1Fe 240/40.

Table 10. Measured and model-calculated temperature using catalogue and identified parameters from the Figure 6.

Duration Time [min]	Temperature [°C]		
	Measured	Model-Calculated	
		Identified Parameters	Catalogue Parameters
18	60.84	60.89	60.93
19	61.54	61.57	61.60
20	61.82	61.83	61.87
21	61.87	61.88	61.92
22	61.76	61.75	61.79
23	61.44	61.45	61.49
24	61.35	61.37	61.41
25	61.14	61.14	61.18
26	60.62	60.62	60.66

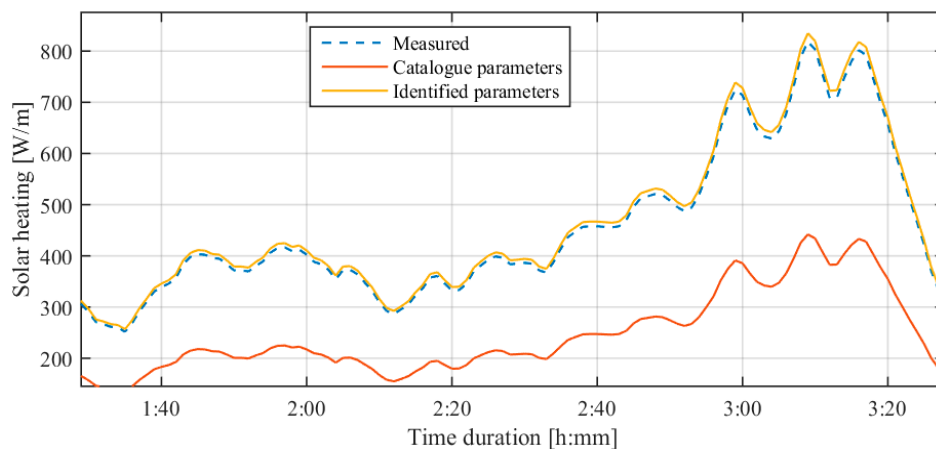


Figure 7. Measured (blue dashed line) and calculated solar heating using catalogue parameters (red line) and parameters determined by the proposed optimization procedure (yellow line).

The comparison between mean and maximum values of measured and dynamic model calculated conductor temperatures, heating and cooling powers, is shown in Table 11 for the conductors' operating temperature around 60 °C. The agreement between measured and calculated results is very good. The deviation between mean and maximum measured and calculated conductor temperature is less than 0.03, which is a great result. Moreover, the deviation between mean and maximum measured and calculated heating and cooling powers is less than 0.14, which is a huge improvement in comparison with the results before optimization, where the deviation was 4.42 (Tables 2 and 3). Thus, the deviation between mean and maximum values has been reduced by 31.6 times.

Table 11. Measured (meas.) and model-calculated (calc.) mean and maximum values of the conductor temperature, heating and cooling powers (per unit values) for conductors AlFe 490/65 and AlFe 240/40 at 60 °C after optimization.

Operating Temperature 60 °C		Mean Value			Maximum Value		
		Meas.	Calc.	Meas. – Calc.	Meas.	Calc.	Meas. – Calc.
AlFe 490/65	T_s [°C]	55.42	55.41	0.01	60.69	60.67	0.02
	P_j [p.u.]	1	1	0	1	1	0
	P_s [p.u.]	1	1.01	0.01	1	1.01	0.01
	P_c [p.u.]	1	0.97	0.03	1	0.97	0.03
	P_r [p.u.]	1	1.14	0.14	1	1.13	0.13
AlFe 240/40	T_s [°C]	56.74	56.74	0	61.87	61.88	0.01
	P_j [p.u.]	1	1	0	1	1	0
	P_s [p.u.]	1	1.01	0.01	1	1.01	0.01
	P_c [p.u.]	1	0.97	0.03	1	0.97	0.03
	P_r [p.u.]	1	1.13	0.13	1	1.13	0.13

The optimization obtained heat equation parameters determined for the conductor temperature around 60 °C were used to compare mean and maximum values of measured and conductor dynamic model calculated conductor temperatures, heating and cooling powers, for the conductor's operating temperature around 80 °C. The results presented in Table 12 show very good agreement between measured and calculated results.

Table 12. Measured (meas.) and model-calculated (calc.) mean and maximum values of the conductor temperature, heating and cooling powers (per unit values) for conductors AlFe 490/65 and AlFe 240/40 at 80 °C after optimization.

Operating Temperature 80 °C		Mean Value			Maximum Value		
		Meas.	Calc.	Meas. – Calc.	Meas.	Calc.	Meas. – Calc.
AlFe 490/65	T_s [°C]	70.85	70.86	0.01	81.08	81.07	0.01
	P_j [p.u.]	1	1	0	1	1	0
	P_s [p.u.]	1	1.01	0.01	1	1.01	0.01
	P_c [p.u.]	1	0.97	0.03	1	0.97	0.03
	P_r [p.u.]	1	1.13	0.13	1	1.14	0.14
AlFe 240/40	T_s [°C]	78.39	78.42	0.03	81.54	81.56	0.02
	P_j [p.u.]	1	1	0	1	1	0
	P_s [p.u.]	1	1.01	0.01	1	1.02	0.02
	P_c [p.u.]	1	0.97	0.03	1	0.97	0.03
	P_r [p.u.]	1	1.14	0.14	1	1.14	0.14

The comparison of measured and model calculated time behaviours of conductor temperatures is shown in the Figures 8 and 9. All performed measurements contain three intervals. In the first and third intervals, there is no current in the conductor, whilst in the second interval constant conductor current is controlled. The three intervals can also be seen clearly in the time behaviours of conductor temperature. The first interval is very short at the very beginning. In the second interval, where constant conductor current is applied, the temperature increases to the operating point and after that keeps almost

constant value. When the current is switched-off at the beginning of the third interval, the conductor temperature starts to decrease.

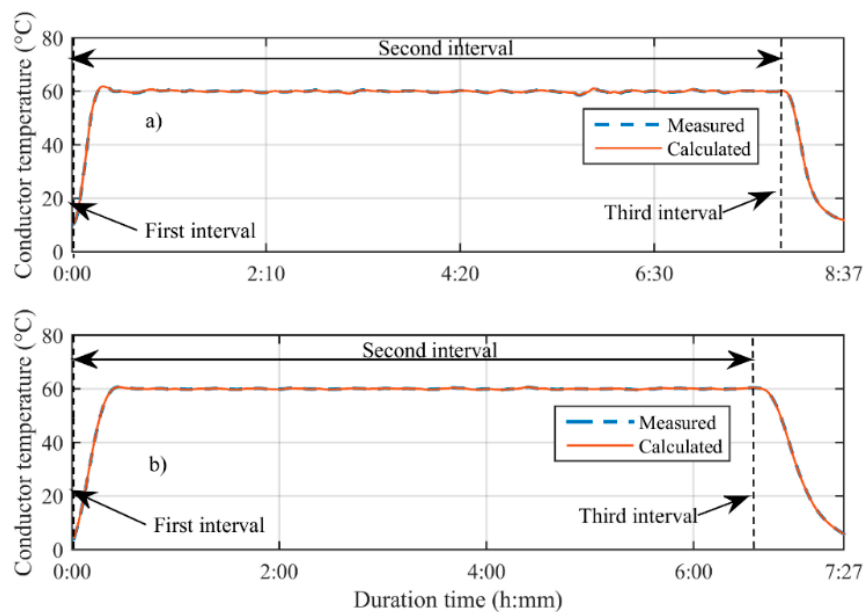


Figure 8. Measured and calculated conductor temperature at the conductor temperature 60 °C for the conductor: (a) AlFe 240/40 and (b) AlFe 490/65.

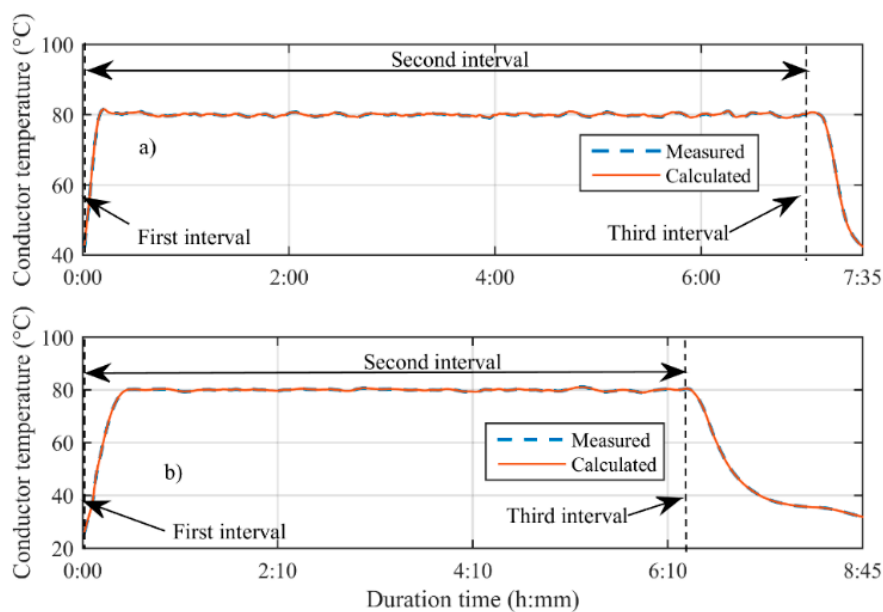


Figure 9. Measured and calculated conductor temperature at the conductor temperature 80 °C for the conductor: (a) AlFe 240/40 and (b) AlFe 490/65.

Figure 8 shows the comparison between measured and model calculated time behaviours of conductor temperature for the conductors AlFe 490/65 and AlFe 240/40 at working temperature around 60 °C. This is the temperature for which the conductor model parameters were determined. In order to confirm the proposed method, the measured and calculated time behaviours of conductor temperature are compared also for the working temperature around 80 °C, using the same model parameters as in the previous case (60 °C). The obtained results are shown in Figure 9.

The results presented in Figures 8 and 9 show a very good agreement between the time behaviours of measured and calculated conductor temperature. Let us check the performance of the proposed parameter determination method and corresponding conductor model in a realistic case, where the conductor temperature is changing all the time. In the given case, the conductor model parameters from Table 9 are applied together with the measured environmental temperature, solar radiation, wind velocity and conductor current. The comparison of measured and calculated conductor temperature is shown in Figure 10 for the conductor AlFe 240/40. These results are completed by the comparison between mean and maximum measured and conductor dynamic model calculated conductor temperature, heating and cooling powers, given in Table 13.

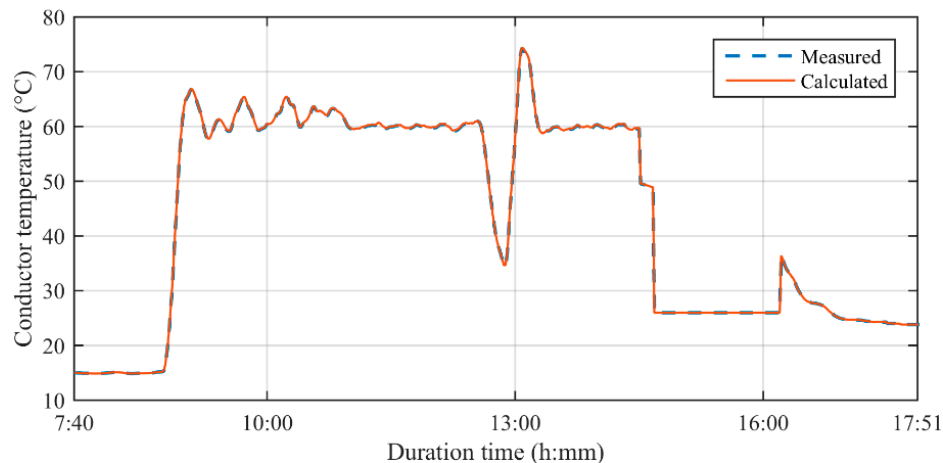


Figure 10. Measured and calculated conductor temperature.

Table 13. Measured (meas.) and model-calculated (calc.) mean and maximum values of the conductor temperature heating and cooling powers (per unit values) for the conductor AlFe 240/40 using heat equation parameters after optimization.

AlFe 240/40 at 60 °C	Mean Value			Maximum Value		
	Meas.	Calc.	Meas. – Calc.	Meas.	Calc.	Meas. – Calc.
T_s [°C]	43.92	43.97	0.05	74.31	74.43	0.12
P_j [p.u.]	1	1	0	1	1	0
P_s [p.u.]	1	1.02	0.02	1	1.02	0.02
P_c [p.u.]	1	0.97	0.03	1	0.97	0.03
P_r [p.u.]	1	1.14	0.14	1	1.14	0.14

The agreement between measured and calculated results shown in Table 13 is very good. The deviation between mean and maximum measured and calculated conductor temperature is less than 0.12. The deviation between mean and maximum measured and calculated heating and cooling powers is less than 0.14, which is a good result.

6. Conclusions

In this paper, the DE has been applied in identifying the parameters of heat equation in order to estimate the temperature of the bare overhead conductor. The main components in the parameters' determination process are the conductor model, measured time behaviours of all relevant variables and DE algorithm. The optimization goal is to find those heat equation parameters, where the difference between the measured and model calculated time behaviour of conductor temperature is minimal. The proposed method requires measured time behaviours of environmental temperature, solar radiation, wind velocity, conductor current and conductor temperature.

The results presented in the paper clearly show that the proposed method for determining the heat equation parameters has to be applied for only one set of measured time behaviours of all variables. The obtained parameters can be afterwards used in the entire range of conductor operation, providing a very good agreement between the measured and calculated time behaviours of conductor temperatures. It is applicable for different operation conditions and for different conductor types.

The proposed method and corresponding model represent a tool that can be applied in critical operating conditions to properly predict maximum acceptable current load of an overhead power line. Moreover, the proposed method also substantially improves the agreement between the model calculated and by measurement determined heating and cooling power, which helps to get a deeper insight into the phenomena responsible for the changes in conductor temperature.

Supplementary Materials: The following is available online at <http://www.mdpi.com/1996-1073/11/8/2061/s1>, Table S1: An example of the input data values.

Author Contributions: All authors contributed equally to all the sections of this work. Writing—Original Draft and Preparation, M.S.; Writing—Review and Editing, J.P., N.S. and G.Š.; Supervision G.Š.

Funding: This research received no external funding.

Conflicts of Interest: The authors declare no conflict of interest.

References

- Muhr, M.; Pack, S.; Jaufer, S.; Haimbl, W.; Messner, A. Experiences with the Weather Parameter Method for the use in overhead line monitoring systems. *Elektrotechnik und Informationstechnik* **2008**, *125*, 444–447. [[CrossRef](#)]
- Gomez, F.A.; de Maria, J.M.G.; Puertas, D.G.; Bairi, A.; Arrabé, R.G. Numerical study of the thermal behaviour of bare overhead conductors in electrical power lines. In *Recent Researches in Communications, Electrical & Computer Engineering*; World Scientific and Engineering Academy and Society (WSEWAS): Montreux, Switzerland, 2011; pp. 149–153.
- Šnajdr, J.; Sedláček, J.; Vostracký, Z. Application of a line ampacity model and its use in transmission lines operations. *J. Electr. Eng.* **2014**, *65*, 221–227. [[CrossRef](#)]
- Wiecek, B.; De Mey, G.; Chatziathanasiou, V.; Papagiannakis, A.; Theodosoglou, I. Harmonic analysis of dynamic thermal problems in high voltage overhead transmission lines and buried cables. *Int. J. Electr. Power Energy Syst.* **2014**, *58*, 199–205. [[CrossRef](#)]
- Theodosoglou, I.; Chatziathanasiou, V.; Papagiannakis, A.; Wiecek, B.; De Mey, G. Electrothermal analysis and temperature fluctuations' prediction of overhead power lines. *Int. J. Electr. Power Energy Syst.* **2017**, *87*, 198–210. [[CrossRef](#)]
- Krontiris, T.; Wasserrab, A.; Balzer, G. Weather-based Loading of Overhead Lines—Consideration of Conductor's Heat Capacity. In Proceedings of the International Symposium of Modern Electric Power Systems, Wroclaw, Poland, 20–22 September 2010; pp. 1–8.
- Jiang, J.A.; Liang, Y.T.; Chen, C.P.; Zheng, X.Y.; Chuang, C.L.; Wang, C.H. On Dispatching Line Ampacities of Power Grids Using Weather-Based Conductor Temperature Forecasts. *IEEE Trans. Smart Grid* **2018**, *9*, 406–415. [[CrossRef](#)]
- Pytlak, P.; Musilek, P.; Lozowski, E.; Toth, J. Modelling precipitation cooling of overhead conductors. *Electr. Power Syst. Res.* **2011**, *81*, 2147–2154. [[CrossRef](#)]
- Yang, Y.; Harley, R.G.; Divan, D.; Habetler, T.G. Overhead conductor thermal dynamics identification by using Echo State Networks. In Proceedings of the International Joint Conference on Neural Networks, Atlanta, GA, USA, 14–19 June 2009; pp. 3436–3443.
- Sidea, D.; Baran, I.; Leonida, T. Weather-based assessment of the overhead line conductors thermal state. In Proceedings of the IEEE Eindhoven PowerTech, Eindhoven, The Netherlands, 29 June–2 July 2015.
- Liu, J.; Yang, H.; Yu, S.; Wang, S.; Shang, Y.; Yang, F. Real-Time Transient Thermal Rating and the Calculation of Risk Level of Transmission Lines. *Energies* **2018**, *11*, 1233. [[CrossRef](#)]
- Wang, Y.; Mo, Y.; Wang, M.; Zhou, X.; Liang, L.; Zhang, P. Impact of Conductor Temperature Time-Space Variation on the Power System Operational State. *Energies* **2018**, *11*, 760. [[CrossRef](#)]

13. CIGRE Working Group 22.12. The Thermal Behaviour of Overhead Conductors Section 1 and 2: Mathematical Model for Evaluation of Conductor Temperature in the Steady State and the Application Thereof. *Electra* **1992**, *4*, 107–125. Available online: https://e-cigre.org/publication/ELT_144_3-the-thermal-behaviour-of-overhead-conductors-sections-1-and-2 (accessed on 7 August 2018).
14. IEEE. *IEEE Std 738-2012: IEEE Standard for Calculating the Current-Temperature Relationship of Bare Overhead Conductors*; IEEE Standard Association: Washington, DC, USA, 2013.
15. CIGRE Working Group B2. 43. *Guide for Thermal Rating Calculations of Overhead Lines*; Technical Brochure 601; CIGRE: Paris, France, 2014; Available online: <https://e-cigre.org/publication/601-guide-for-thermal-rating-calculations-of-overhead-lines> (accessed on 7 August 2018).
16. Schmidt, N.P. Comparison between IEEE and CIGRE ampacity standards. *IEEE Trans. Power Deliv.* **1999**, *14*, 1555–1559. [[CrossRef](#)]
17. Arroyo, A.; Castro, P.; Martinez, R.; Manana, M.; Madrazo, A.; Lecuna, R.; Gonzalez, A. Comparison between IEEE and CIGRE Thermal Behaviour Standards and Measured Temperature on a 132-kV Overhead Power Line. *Energies* **2015**, *8*, 13660–13671. [[CrossRef](#)]
18. Zhan, Q.; Wu, S.; Li, Q. A PSO identification algorithm for temperature adaptive adjustment system. In Proceedings of the IEEE International Conference on Industrial Engineering and Engineering Management (IEEM), Singapore, 6–9 December 2015.
19. Meenal, R.; Selvakumar, A.I. Temperature based model for predicting global solar radiation using genetic algorithm [GA]. In Proceedings of the International Conference on Innovations in Electrical, Electronics, Instrumentation and Media Technology (ICEEIMT), Coimbatore, India, 3–4 February 2017.
20. Marčić, T.; Štumberger, G.; Štumberger, B.; Hadžiselimović, M.; Vrtič, P. Determining parameters of a line-start interior permanent magnet synchronous motor model by the differential evolution. *IEEE Trans. Magn.* **2008**, *44*, 4385–4388. [[CrossRef](#)]
21. Glotic, A.; Pihler, J.; Ribic, J.; Stumberger, G. Determining a gas-discharge arrester model's parameters by measurements and optimization. *IEEE Trans. Power Deliv.* **2010**, *25*, 747–754. [[CrossRef](#)]
22. Sarajlić, M.; Pocajt, M.; Kitak, P.; Sarajlić, N.; Pihler, J. Covered overhead conductor temperature coefficient identification using a differential evolution optimization algorithm. *B&H Electr. Eng.* **2017**, *11*, 26–35.
23. Storn, R.; Price, K. Differential Evolution—A Simple and Efficient Heuristic for global Optimization over Continuous Spaces. *J. Glob. Optim.* **1997**, *11*, 341–359. [[CrossRef](#)]
24. Sarajlić, M.; Kitak, P.; Pihler, J. New design of a medium voltage indoor post insulator. *IEEE Trans. Dielectr. Electr. Insul.* **2017**, *24*, 1162–1168. [[CrossRef](#)]
25. Glotic, A.; Sarajlic, N.; Kasumovic, M.; Tesanovic, M.; Sarajlic, M.; Pihler, J. Identification of thermal parameters for transformer FEM model by differential evolution optimization algorithm. In Proceedings of the International Conference Multidisciplinary Engineering Design Optimization, Belgrade, Serbia, 14–16 September 2016. [[CrossRef](#)]
26. Sarajlić, M.; Pihler, J.; Sarajlić, N.; Kitak, P. Electric Field of a Medium Voltage Indoor Post Insulator. In *Electric Field*, 1st ed.; Sheikholeslami, M.K., Ed.; IntechOpen: London, UK, 2018; pp. 145–159.
27. Price, K.V.; Storn, R.M.; Lampinen, J.A. *Differential Evolution—A Practical Approach to Global Optimization*, 1st ed.; Springer-Verlag: Berlin/Heidelberg, Germany, 2005. [[CrossRef](#)]
28. Kiessling, F.; Nefzger, P.; Nolasco, J.F.; Kaintzyk, U. *Overhead Power Lines: Planning, Design, Construction*; Springer: Berlin, Germany, 2003.
29. Technical Data for Aluminium-Steel Rope for Overhead Line. Available online: http://www.tim-kabel.hr/images/stories/katalog/datasheetHRV/0602_ACSR_ENG.pdf (accessed on 11 July 2018).

